Research Article

Valmik Madhav Mahajan*, and Amit Sharma

Evaluation of static responses for layered composite arches

Abstract: Layered composite materials are widely used across a variety of sectors, including the automotive industry, aerospace engineering, offshore, and various mechanical domains, because of their strong yet light-weight structures. Therefore, various emergent theories are available on the deformation of layered beams. The previous research studies are insufficient as they are based on deformation of layered composite and sandwich arches with simply supported (SS) end conditions. Therefore, it is a good opportunity for researchers to investigate the arches using exponential shear deformation and normal deformation theory. The leading hypothesis mainly adds to the research of bending for sandwich and layered composite arches adopting the exponential theory. The present theory does not require any shear correction factor to satisfy zero transverse shear stress condition at the bottom and top fibers of arches. Governing equations and associated end conditions are derived through principle of virtual work. Navier's techniques used for sandwich and layered composite arches are SS boundary conditions subjected to uniformly distributed load. The results of the current study showed that the exponential normal and shear deformation theories may be used to evaluate static responses for layered composite and sandwich arches. The obtained results from the present theory are validated through the results available in published literature.

Keywords: arches, exponential, layered composite, sandwich, static responses, bending

---

* **Corresponding author: Valmik Madhav Mahajan,** Department of Civil Engineering, Oriental University, Indore-453555, Madhya Pradesh, India, e-mail: valmikmahajan001@gmail.com
Amit Sharma: Department of Civil Engineering, Oriental University, Indore-453555, Madhya Pradesh, India, e-mail: sgsitsamit25@gmail.com

1 Introduction

Composite materials are extensively used in various industries such as aerospace, marine structures, various mechanical domain, offshore, ship building industries, automobile sectors, and also broadly used in the field of civil engineering due to their superior properties, *viz*, more strength, high stiffness-to-weight ratio, and good fatigue resistance. The demand for smart and lightweight structures is increasing these days. It is required to develop a precise solution with higher order for evaluation of static and vibration responses of layered composite as well as sandwich arches subjected to uniformly distributed load. Development of various beam theories has been formulated in few eras. The sufficient literature is available on straight beams for different responses and for various loading conditions. Bernoulli–Euler established the first beam theory called the "Classical beam theory" (CBT). The thickness stretching effect is ignored in the well-known theories such as CBT and Bernoulli–Euler theory [1,2].

Later on, CBT was modified by Timoshenko [3,4] with the consideration of shear deformation effect, but it required shear correction factor which contributed constant behavior shear-strain through the thickness. Timoshenko has accounted shear deformation in his developed theory which is well-known as "first-order shear deformation theory" (FSDT) and this theory is universally known as "Timoshenko beam theory" (TBT) in the year of 1921. Recently, higher order theories were represented on bending responses, buckling responses, free-vibration responses for layered composite, functionally graded sandwich beams by Sayyad and his co-authors [5–7]. The inadequacy of CBT as well as TBT was the basement of advance in various refined theories. Some higher order shear deformation theories (HSDTs) are published by researchers accounting transverse shear deformation. Those HSDTs are classified as layer wise, zigzag, and equivalent single layer wise theories.

Several refined theories were invented by Kant and Manjunath [8] for sandwich and layered composite beams with C^O finite element application. The responses for layered composite beams in the form of finite element C^O in zig-zag

pattern were developed by Aitharaju and Averill [9]. Then, Reddy [10] developed the popularly named third-order shear deformation theory for layered composite plate, which is used for various lamination schemes. This work was extended by Khdeir and Reddy [11,12] in 1997 based on static analysis for thick layered and thin layered cross-ply composite beams and discovered an exact solution.

Carrera [13–15] addressed the effect of thermal stress responses and transverse normal stress for multilayered shells and plates. Variational approach of Maupertuis-Lagrange was applied for layered composite using refined higher order theory by Zenkour [16]. An accurate theory was developed on bending responses using hyperbolic shear deformation theory for thick beams [17] and for sandwich beams using functionally graded materials by Sayyad and his co-authors [18,19]. Few literature are available on functionally graded sandwich curved beams and optimum solution was addressed by Avhad and Sayyad [20,21] on the effectiveness of static responses.

In the last decade, Tornabene *et al.* [22] had used refined shear deformation theories for laminated composite beams and arches considering the thickness as a main variable and also investigated the seismic capacity by considering the parametric investigation for masonry arches and portals of various shapes [23]. They have used the generalized differential quadrature [24] method and found a very good agreement which demonstrates the feasibility and performance of dynamic modeling for arches. The authors also studied the seismic response of vaulted and arched structures made of composite/isotropic materials [25].

Present theory deals with the static responses for sandwich and layered composite arches using exponential normal deformation and shear deformation theory. It is acquainted that strain deformation is not considered in existing HSDTs and other theories. Therefore, the present theory includes strain deformation as well as normal deformation effect, *i.e.*, thickness stretching. The present theory contribution is very important in this research area and very few researchers are working on analysis of anti-symmetric two-layered, symmetric three-layered composite arches and sandwich arches subjected to uniformly distributed load (UDL).

1.1 Motivation

As authors noticed that very limited literature is available on arches, this motivated the authors for further investigation using novel exponential shear and normal deformation

theory for sandwich and layered arches. Arches are commonly used in many civil engineering structures for aesthetic purposes. Due to the increases in smart, lightweight, and architectural demands, it is very necessary to use arches using sandwich and layered composite materials for such constructions. This is good and attractive material with unique properties.

1.2 Novelty and main contributions

1. Arches in elevation has curvature in effect, which are widely used in construction fields such as RCC buildings, convention/building centers, arch-type bridges, pipe bends, curved/arches segment of machine tool frames, chain links, cement silos, *etc.*, where circular/arches serve the purpose in the form of ring beams. Several arches type of segments uses in different industries are frequently subjected static-forces wherever needs to design and analyze precisely. This will create the interest for researchers to choose the research area for investigation purpose.
2. As per the available literature, it is noticed that vast literature are available on straight beams, but only very limited literature are available on arches which accounts for the transverse deformation effect.
3. The major contributions of present study includes the effect of transverse shear and normal deformation, i.e., thickness stretching and hence, this is the novelty of present investigation.
4. The present theory well captures the responses for layered composite and sandwich arches using exponential theory.
5. The present theory satisfied the zero transverse shear stress simply supported (SS) boundary conditions at top fiber and bottom surface of the arches without using the problematic reliant shear correction factor.

2 Mathematical formulation for layered composite and sandwich arches

Consider the layered composite and sandwich arches with curvature radius "R" shown in Figure 1. The beam x, y, and z-axes are taken horizontally along the length (L), unit width (b), and the total thickness (h) of the arches, respectively. The arches are rectangular in cross

section as $b \times h$. The z-axis is considered as downward (+ve) positive. The layered composite arches are subjected to vertical UDL and denoted by symbol q, where b = unit width of arches ($b = 1.0$), h = total thickness of arches ($0 \leq x \leq L$; $-b/2 \leq y \leq b/2$; $-h/2 \leq z \leq h/2$).

The arches made up of multilayered composite material are placed one above the other according to various lamination schemes for layered composite arches, i.e., 0°/90°/0° and 0°/90° and sandwich arches, i.e., 0°/Core/0°. Good quality and very strong glue can be applied between any two adjacent layers of 0 (zero) thickness to prevent delamination. The detailed geometry for antisymmetric two-layered, symmetric three-layered composites and sandwich arches are subjected to UDL as given below.

2.1 Displacement field

Displacement field in terms of normal and shear deformations for present theory is stated as follows:

$$u(x, z) = \left(1 + \frac{z}{R}\right)u_0 - z\frac{\partial w_0}{\partial x} + f(z)\phi \quad \text{and}$$
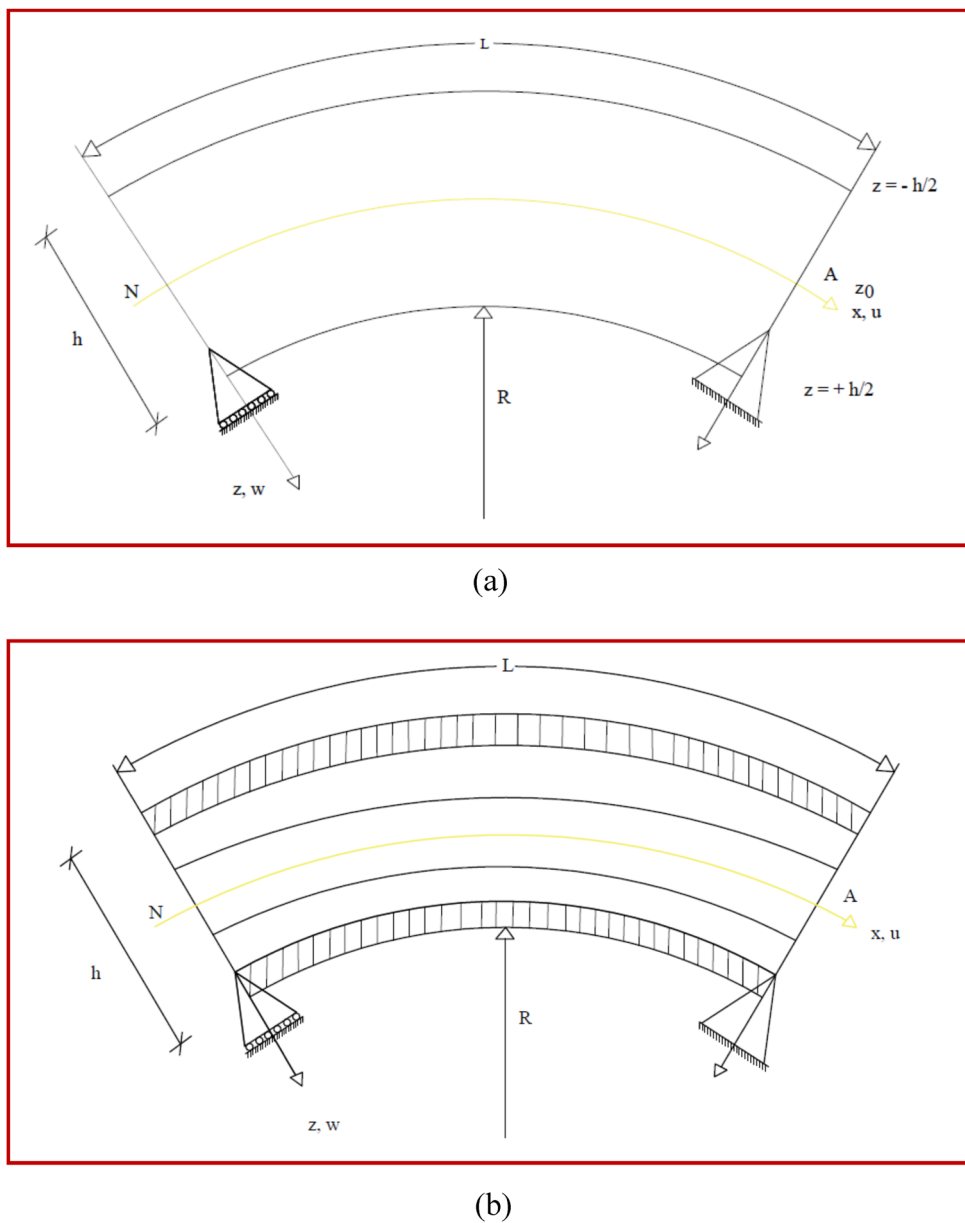$$w(x, z) = w_0 + f'(z)\psi, \tag{1}$$

(a)

(b)

Figure 1: Geometry of (a) two-layered composite arches subjected to UDL and (b) sandwich arches subjected to UDL.

where u_0, w_0, ϕ, and ψ are four unknown displacement functions at mid-plane for arches. $f(z)$ and $f'(z)$ represent the function in terms of shear and normal deformations through the thickness of arches subjected to UDL.

When "w" is a function of "z," cartesian coordinates are commonly well known as transverse displacements. Transverse normal strain through the thickness of arches is not equal to zero, *i.e.*, $\varepsilon_z \neq 0$. The displacement field recommended in Eq. (1) is purely based on 2D reactions of the plate. But in 1D arches, the rotation about the y-direction is assumed to be zero (0) and the breadth of arches is considered as unity or unit width. Hence, displacements in breadth direction are eliminated. For the present theory sandwich and layered arches, non-zero strain (ε_z) components are calculated using the following relationship of strain−displacement based on elasticity theory:

$$\varepsilon_x^k = \frac{\partial u}{\partial x} + \frac{w}{R}, \tag{2}$$

$$\varepsilon_z^k = \frac{\partial w}{\partial z}, \tag{3}$$

$$\gamma_{xz}^k = \frac{\partial u}{\partial z} + \frac{\partial w}{\partial x} - \frac{u_0}{R}. \tag{4}$$

By using displacement field given in Eq. (1), finding the expression for normal strain about both the axes and the transverse shear strain considered at any point on the arches is given as follows:

$$\varepsilon_x^k = \frac{\partial u_0}{\partial x} - z\frac{\partial^2 w_0}{\partial x^2} + f(z)\frac{\partial \phi}{\partial x} + \frac{w_0}{R} + \frac{f'(z)}{R}\psi, \tag{5}$$

$$\varepsilon_z^k = f''(z)\psi, \tag{6}$$

$$\gamma_{xz}^k = f'(z)\left(\phi + \frac{\partial \psi}{\partial x}\right), \tag{7}$$

where

$$f(z) = ze^{-2(z/h)^2}, \tag{8}$$

$$f'(z) = e^{-2(z/h)^2}\left(1 - \frac{4\,z^2}{h^2}\right), \tag{9}$$

$$f''(z) = e^{-2(z/h)^2}\left(\frac{16z^3 - 12zh^2}{h^4}\right), \tag{10}$$

where single dash symbol represents the derivatives with respect to z. According to the present theory, $\varepsilon_z \neq 0$ indi-

cates the current research article accounting the transverse normal deformation/strain effect. Several recognized theories have ignored this type of effect as represented in Table 1.

2.2 Constitutive relations

A 2D Hooke's law is used to obtain the expression of bending and shear stresses for layered composite and sandwich arches. The variations in stress-strain in the form of kth layer wise laminate principle axes (x, z) and material reference axes (1, 3), respectively, are given as follows:

$$\begin{Bmatrix} \sigma_x \\ \sigma_z \\ \tau_{xz} \end{Bmatrix}^k = \begin{bmatrix} Q_{11} & Q_{13} & 0 \\ Q_{13} & Q_{33} & 0 \\ 0 & 0 & Q_{55} \end{bmatrix}^k \begin{Bmatrix} \varepsilon_x \\ \varepsilon_z \\ \gamma_{xz} \end{Bmatrix}^k, \tag{11}$$

$$\{\sigma\}^k = [Q_{ij}]^k\{\varepsilon\}^k,$$

where $\{\sigma\}^k$ represents the normal stresses with respect to (x, z) axes called as stress quantity, $\{\varepsilon\}^k$ is the transverse shear stress along "x–z" plane called as strain quantity, and $[Q_{ij}]^k$ is the reduced stiffness coefficient known as transformed rigidity matrix.

The elements of the above transformed rigidity matrix are given below.

$$Q_{11} = \left(\frac{E_1^k}{1 - (\mu_{13}\mu_{31})}\right),$$

$$Q_{13} = \left(\frac{E_3^k\mu_{13}}{1 - (\mu_{13}\mu_{31})}\right),$$

$$Q_{33} = \left(\frac{E_3^k}{1 - (\mu_{13}\mu_{31})}\right), \tag{12}$$

$$Q_{44} = G_{23}^k,$$

$$Q_{55} = G_{13}^k,$$

where μ_{13} and μ_{31} are the Poisson's ratio, E_1^k and E_3^k are the elasticity modulus about (1, 3) laminate plane, and G_{13}^k and G_{23}^k are the shear modulus of lamina.

The normal stresses are determined using Hooke's law as follows:

$$\sigma_x^k = Q_{11}\varepsilon_x + Q_{13}\varepsilon_z, \tag{13}$$

Table 1: Confirmation of effect of normal deformation (ε_z) and shear deformation (γ_{xz})

S. No.	ε_z	γ_{xz}	Sources
1	$\varepsilon_z = 0$	$\gamma_{xz} = 0$	Bernoulli [1] and Euler [2]
2	$\varepsilon_z = 0$	$\gamma_{xz} \neq 0$ or $\gamma_{zx} \neq 0$	Timoshenko [3,4]; Sayyad and Ghugal [5]; Kant and Manjunath [8]; Reddy [10]

$$\sigma_z^k = Q_{13}\,\varepsilon_x + Q_{33}\,\varepsilon_z, \tag{14}$$

$$\tau_{xz}^k = Q_{55}\,\gamma_{xz}, \tag{15}$$

$$\varepsilon_y^k = \gamma_{xy}^k = \gamma_{yz}^k = 0. \tag{16}$$

2.3 Application of virtual work principle

Governing equations with traction-free SS boundary conditions are obtained using the principle of virtual work stated below in Eq. (17).

Using principle of virtual work, we know that
Internal work done – External work done = 0

$$\therefore \int_0^L \int_{-h/2}^{+h/2} (\sigma_x^k \delta\varepsilon_x + \sigma_z^k \delta\varepsilon_z + \tau_{xz}^k \delta\gamma_{xz})dxdz$$
$$- \int_0^L (q\delta w dx) = 0, \tag{17}$$

where "δ" is the variational operator.

Eq. (17) can be represented as follows by using shear deformation and normal deformation using Eqs. (2)–(4).

We have

$$[L_{33}] = Q_{33} \int_{-h/2}^{+h/2} [f''(z)^2]\,dz, \tag{23}$$

$$[J_{55}] = Q_{55} \int_{-h/2}^{+h/2} [f'(z)^2]\,dz. \tag{24}$$

These integration constants are generally used while axial-displacements, transverse-displacements, bending stresses, and shear stresses result through the thickness in x–z plane. The present theory used free SS boundary conditions at the top fiber and bottom surface of ($x = 0$, $x = L$) arches. The present theory used MATLAB 2015 to write the codes for layered composite and sandwich arches based on theoretical formulation.

The four governing equations in the form of unknown variables (u_0, w_0, ϕ, and ψ) and integration constants are obtained as follows:

$$\delta u_0 : -A_{11}\frac{\partial^2 u_0}{\partial x^2} + B_{11}\frac{\partial^3 w_0}{\partial x^3} - \frac{A_{11}}{R}\frac{\partial w_0}{\partial x} - C_{11}\frac{\partial^2 \phi}{\partial x^2}$$
$$- \left(\frac{D_{11}}{R} + L_{13}\right)\frac{\partial \psi}{\partial x} = 0, \tag{25}$$

$$\int_{-h/2}^{+h/2}\int_0^L (\sigma_x^k \delta\varepsilon_x)dxdz = \int_{-h/2}^{+h/2}\int_0^L \left[Q_{11}\left(\frac{\partial u_0}{\partial x} - z\frac{\partial^2 w_0}{\partial x} + f(z)\frac{\partial \phi}{\partial x} + \frac{w_0}{R} + \frac{f'(z)}{R}\psi\right) + Q_{13}(f''(z))\psi\right]$$
$$\star \left[\frac{\partial \delta u_0}{\partial x} - z\frac{\partial^2 \delta w_0}{\partial x} + f(z)\frac{\partial \delta\phi}{\partial x} + \frac{\delta w_0}{R} + \frac{f'(z)}{R}\delta\psi\right]dxdz, \tag{18}$$

$$\int_{-h/2}^{+h/2}\int_0^L (\sigma_z^k \delta\varepsilon_z)dxdz = \int_{-h/2}^{+h/2}\int_0^L \left\{\left[Q_{13}\left(\frac{\partial u_0}{\partial x} - z\frac{\partial^2 w_0}{\partial x} + f(z)\frac{\partial \phi}{\partial x} + \frac{w_0}{R} + \frac{f'(z)}{R}\psi\right) \atop + Q_{33}(f''(z))\psi\right][f''(z)\delta\psi]\right\}dxdz, \tag{19}$$

$$\int_{-h/2}^{+h/2}\int_0^L (\tau_{xz}^k \delta\gamma_{xz})dxdz = \int_{-h/2}^{+h/2}\int_0^L \left\{\left[Q_{55}f'(z)\left(\phi + \frac{\partial \psi}{\partial x}\right)\right]\left[f'(z)\left(\delta\phi + \frac{\partial \delta\psi}{\partial x}\right)\right]\right\}dxdz. \tag{20}$$

Integrating Eqs. (18)–(20) by parts rule, and accumulating the coefficients of δu_0, δw_0, $\delta\phi$, and $\delta\psi$, set them equal to zero. Integration stiffness constants appearing in Eqs. (18)–(20) is given below as follows:

$$[A_{11},\ B_{11},\ C_{11},\ D_{11},\ E_{11},\ F_{11},\ G_{11},\ H_{11},\ I_{11},\ J_{11}] = Q_{11} \int_{-h/2}^{+h/2} \begin{bmatrix} 1,\ z,\ f(z),\ f'(z),\ z^2,\ zf(z), \\ zf'(z),\ f(z)^2,\ f(z)f'(z),\ f'(z)^2 \end{bmatrix} dz, \tag{21}$$

$$[L_{13},\ M_{13},\ N_{13},\ O_{13}] = Q_{13} \int_{-h/2}^{+h/2} [f''(z),\ z\,f''(z),\ f(z)f''(z),\ f'(z)f''(z)]dz, \tag{22}$$

$$\delta w_0 : -B_{11}\frac{\partial^3 u_0}{\partial x^3} + \frac{A_{11}}{R}\frac{\partial u_0}{\partial x} + E_{11}\frac{\partial^4 w_0}{\partial x^4}$$
$$- 2\frac{B_{11}}{R}\frac{\partial^2 w_0}{\partial x^2} + \frac{A_{11}}{R^2}w_0 - F_{11}\frac{\partial^3 \phi}{\partial x^3} + \frac{C_{11}}{R}\frac{\partial \phi}{\partial x}$$
$$+ \left(\frac{D_{11}}{R^2} + \frac{L_{13}}{R}\right) \quad (26)$$
$$\psi - \left(\frac{G_{11}}{R} + M_{13}\right)\frac{\partial^2 \psi}{\partial x^2} = q_0,$$

$$\delta\phi : -C_{11}\frac{\partial^2 u_0}{\partial x^2} + F_{11}\frac{\partial^3 w_0}{\partial x^3} - \frac{C_{11}}{R}\frac{\partial w_0}{\partial x} + J_{55}\phi$$
$$- H_{11}\frac{\partial^2 \phi}{\partial x^2} - \frac{I_{11}}{R}\frac{\partial \psi}{\partial x} - N_{13}\frac{\partial \psi}{\partial x} + J_{55}\frac{\partial \psi}{\partial x} = 0, \quad (27)$$

$$\delta\psi : \left(\frac{D_{11}}{R} + L_{13}\right)\frac{\partial u_0}{\partial x} + \left(\frac{D_{11}}{R^2} + \frac{L_{13}}{R}\right)w_0$$
$$- \left(\frac{G_{11}}{R} + M_{13}\right)\frac{\partial^2 w_0}{\partial x^2} + \frac{I_{11}}{R}\frac{\partial \phi}{\partial x} + N_{13}\frac{\partial \phi}{\partial x}$$
$$- J_{55}\frac{\partial \phi}{\partial x} + \frac{J_{11}}{R}\psi + 2\frac{O_{13}}{R}\psi + L_{33}\psi \quad (28)$$
$$- J_{55}\frac{\partial^2 \psi}{\partial x^2} = 0.$$

Using the above governing equations normalized bending responses, non-dimensional transverse displacements, normalized axial displacements, and non-dimensional transverse shear stresses can be accomplished for layered composite and sandwich arches. The governing equations for straight beams are obtained by setting their curvature radius of arches to ∞ (infinity).

2.4 Navier's solution techniques

Navier's solution technique is the simplest approach to obtain displacements and stresses for SS end boundary conditions. In the present research article, static responses of SS sandwich and layered composite arches are presented. The given arches have following SS end boundary conditions:

$$x = 0, x = L, \text{ and } u_0 = w_0 = \phi = \psi = 0. \quad (29)$$

Using Navier's solution, unknown variables in displacement field are prolonged in the form of trigonometric series which satisfy the SS boundary conditions indicated in Eq. (29). Trigonometric form considered for unknown variables are stated as follows:

$$u_0 = \sum_{m=1}^{\infty} u_m \cos(\alpha x), \quad (30)$$

$$w_0 = \sum_{m=1}^{\infty} w_m \sin(\alpha x), \quad (31)$$

$$\phi = \sum_{m=1}^{\infty} \phi_m \cos(\alpha x), \quad (32)$$

$$\psi = \sum_{m=1}^{\infty} \psi_m \sin(\alpha x), \quad (33)$$

$$q_0 = q_m \sin(\alpha x), \left(\because \alpha = \frac{m\pi}{L}\right), \quad (34)$$

where u_m, w_m, ϕ_m, and ψ_m are unknown coefficients, which will be determined.

The transverse distributed loading is given as follows:

$$q(x) = \sum_{m=1}^{\infty} \frac{4q_0}{m\pi} \sin(\alpha x)(\because m = 1, 3, 5, 7..... \infty) \quad (35)$$

for UDL,

where q_0 is the maximum intensity of UDL, m is the +ve integer variable with the odd number ($m = 1, 3, 5, 7......\infty$).

By substituting transverse load from Eq. (35) and the unknown variable from Eqs. (30)–(34) in Eqs. (25)–(28) of the governing equations, the bending responses for arches or static solution represented in matrix are obtained as follows:

$$[K]\{\Delta\} = \{f\}, \quad (36)$$

where $[K]$ is the stiffness matrix, $\{\Delta\}$ is the unknown variable, and $\{f\}$ is the force vector.

$$[K] = \begin{bmatrix} A_{11}\alpha^2 & -\left(\frac{A_{11}}{R}\alpha + B_{11}\alpha^3\right) & C_{11}\alpha^2 & -\left(\frac{D_{11}}{R}\alpha + L_{13}\alpha\right) \\ -\left(\frac{A_{11}}{R}\alpha + B_{11}\alpha^3\right) & \left(\frac{A_{11}}{R^2} + 2\frac{B_{11}}{R}\alpha^2 + E_{11}\alpha^4\right) & -\left(\frac{C_{11}}{R}\alpha + F_{11}\alpha^3\right) & \left(\frac{D_{11}}{R^2} + \frac{L_{13}}{R}\right) + \left(\frac{G_{11}}{R}\alpha^2 + M_{13}\alpha^2\right) \\ C_{11}\alpha^2 & -\left(\frac{C_{11}}{R}\alpha + F_{11}\alpha^3\right) & (H_{11}\alpha^2 + J_{55}) & -\left(\frac{I_{11}}{R}\alpha + N_{13}\alpha - J_{55}\alpha\right) \\ -\left(\frac{D_{11}}{R}\alpha + L_{13}\alpha\right) & \left(\frac{D_{11}}{R^2} + \frac{L_{13}}{R}\right) + \left(\frac{G_{11}}{R}\alpha^2 + M_{13}\alpha^2\right) & -\left(\frac{I_{11}}{R}\alpha + N_{13}\alpha - J_{55}\alpha\right) & \left(\frac{J_{11}}{R^2} + 2\frac{O_{13}}{R} + L_{33} + J_{55}\alpha^2\right) \end{bmatrix}, \quad (37)$$

Table 2: Material properties of antisymmetric two-layered, symmetric three-layered composite, and sandwich arches

Material	Elastic/substantial properties	Sources
Present theory	Modulus of elasticity = E_1 = 172.40 GPa, $E_2 = E_3$ = 6.890 GPa, μ_{13} = 0.25, μ_{31} = find according to Poisson's ratio, Shear modulus = $G_{12} = G_{13}$ = 3.450 GPa, G_{23} = 1.378 GPa, ρ = constant Modulus of elasticity = $E_1 = E_2$ = 0.276 GPa, E_3 = 3.450 GPa, μ_{13} = 0.25, shear modulus = G_{12} = 0.1104 GPa, G_{23} = G_{13} = 0.414 GPa, ρ = constant	Kant *et al.* 2007 [26]

$$\{\Delta\} = \begin{Bmatrix} u_m \\ w_m \\ \phi_m \\ \psi_m \end{Bmatrix}, \tag{38}$$

$$\{f\} = \begin{Bmatrix} 0 \\ q_m \\ 0 \\ 0 \end{Bmatrix}. \tag{39}$$

3 Illustrative numerical results and discussion

Numerical results for those problems are mentioned in Tables 3–5 and the same are graphically represented in Figures 2–4 followed by consequent discussion. This section consists of three types of numericals based on various lamination schemes. The present theory including the static responses for layered composite and sandwich arches with SS end boundary conditions are represented to prove the effectiveness and accurateness of the results.

More literature are available on the various kinds of straight beams and many researchers have validated their results using different theories. But limited numerical results are available on curved beams. Therefore, the present theory endorses or validates the results of experiments carried out with straight beam by Reddy [10], Kant *et al.* [26], and Sayyad and Ghugal [27], and that with curved beam by Avhad and Sayyad [28]. The present theory includes mainly three types of lamination schemes such as symmetric three-layered (0°/90°/0°) composite,

Table 3: Assessment of non-dimensional transverse shear stresses, axial displacements, transverse displacements, and axial bending stresses for antisymmetric two-layered (0°/90°) composite arches

L/h	R/h	Theory	$\bar{\tau}_{xz}$	$\bar{u}$	$\bar{w}$	$\bar{\sigma}_x$
4	5	Present theory ($\varepsilon_z \neq 0$)	3.7633	5.7850	5.5285	36.7345
		Avhad and Sayyad [28]	3.6812	5.7738	5.8578	40.9198
	10	Present theory ($\varepsilon_z \neq 0$)	3.6772	4.0714	5.4467	40.2753
		Avhad and Sayyad [28]	3.6832	4.0330	5.8565	40.9294
	20	Present theory ($\varepsilon_z \neq 0$)	3.6569	3.1849	5.4300	40.8242
		Avhad and Sayyad [28]	3.6851	3.0898	5.8571	40.9363
	∞	Present theory ($\varepsilon_z \neq 0$)	3.6502	2.2678	5.4290	40.5816
		Avhad and Sayyad [28]	3.6860	2.0979	5.8578	40.9352
		Reddy [10]	5.0240	2.2580	5.5900	40.2390
		Kant *et al.* [26]	3.8480	—	5.9000	36.6780
		Sayyad and Ghugal [27]	5.0780	2.2680	5.5230	40.4940
10	5	Present theory ($\varepsilon_z \neq 0$)	10.0005	246.3853	3.6978	55.4861
		Avhad and Sayyad [28]	8.9175	248.0907	3.7370	219.8111
	10	Present theory ($\varepsilon_z \neq 0$)	9.8561	142.7770	3.6634	184.3570
		Avhad and Sayyad [28]	8.9175	144.7630	3.7381	219.8409
	20	Present theory ($\varepsilon_z \neq 0$)	9.8230	87.6075	3.6583	214.0700
		Avhad and Sayyad [28]	8.9178	88.5963	3.7381	219.8508
	∞	Present theory ($\varepsilon_z \neq 0$)	9.8138	29.7401	3.6610	221.1290
		Avhad and Sayyad [28]	8.9181	29.4110	3.7390	219.8585
		Reddy [10]	11.5440	29.8050	3.6970	221.0170
		Kant *et al.* [26]	10.7380	—	3.7440	217.3300
		Sayyad and Ghugal [27]	11.5860	29.7990	3.6830	221.4020

Table 4: Assessment of non-dimensional transverse shear stresses, axial displacements, transverse displacements, and axial bending stresses for symmetric three layered (0°/90°/0°) composite arches

L/h	R/h	Theory	$\bar{\tau}_{xz}$	$\bar{u}$	$\bar{w}$	$\bar{\sigma}_x$
4	5	Present theory ($\varepsilon_z \neq 0$)	1.7377	3.2761	3.4082	16.3624
		Avhad and Sayyad [28]	1.9855	3.5159	3.5166	22.2994
	10	Present theory ($\varepsilon_z \neq 0$)	1.7377	2.3050	3.4082	19.7018
		Avhad and Sayyad [28]	1.9852	2.5155	3.5151	22.3754
	20	Present theory ($\varepsilon_z \neq 0$)	1.7377	1.7766	3.4081	20.5487
		Avhad and Sayyad [28]	1.9850	1.9712	3.5151	22.4434
	∞	Present theory ($\varepsilon_z \neq 0$)	1.7377	1.2196	3.4081	20.8469
		Avhad and Sayyad [28]	1.9848	1.3976	3.5151	22.5115
		Reddy [10]	1.8310	1.1620	3.3680	19.6710
		Kant et al. [26]	2.4880	—	3.6050	21.5840
		Sayyad and Ghugal [27]	1.7610	1.1950	3.3940	20.2880
10	5	Present theory ($\varepsilon_z \neq 0$)	4.5073	77.0478	1.1134	30.4639
		Avhad and Sayyad [28]	5.6263	78.7989	1.1345	88.1728
	10	Present theory ($\varepsilon_z \neq 0$)	4.5073	46.2877	1.1134	72.3400
		Avhad and Sayyad [28]	5.6255	47.4498	1.1346	88.1083
	20	Present theory ($\varepsilon_z \neq 0$)	4.5073	29.5506	1.1134	82.8055
		Avhad and Sayyad [28]	5.6249	30.3921	1.1346	88.0762
	∞	Present theory ($\varepsilon_z \neq 0$)	4.5073	11.9087	1.1134	86.2894
		Avhad and Sayyad [28]	5.6243	12.4121	1.1346	88.0442
		Reddy [10]	6.0900	11.7340	1.0980	85.0300
		Kant et al. [26]	6.1500	—	1.1710	89.1200
		Sayyad and Ghugal [27]	6.0160	11.8190	1.1060	85.6640

Table 5: Assessment of non-dimensional transverse shear stresses, axial displacements, transverse displacements, and axial bending stresses for sandwich (0°/Core/0°) arches

| L/h	R/h	Theory	$\bar{\tau}_{xz}$	$\bar{u}$	$\bar{w}$	$\bar{\sigma}_x$
4	5	Present theory ($\varepsilon_z \neq 0$)	3.3532	11.705	12.1668	40.1124
		Avhad and Sayyad [28]	2.0462	9.8338	12.0776	40.1524
	10	Present theory ($\varepsilon_z \neq 0$)	3.3534	7.5701	12.1666	40.1429
		Avhad and Sayyad [28]	2.0462	6.3123	12.0777	40.1892
	20	Present theory ($\varepsilon_z \neq 0$)	3.3534	5.3202	12.1665	40.1672
		Avhad and Sayyad [28]	2.0462	4.3962	12.0777	40.2073
	∞	Present theory ($\varepsilon_z \neq 0$)	3.3534	2.9486	12.1665	40.1853
		Avhad and Sayyad [28]	2.0462	2.3764	12.0777	40.2254
		Reddy [10]	2.6620	2.3650	12.4550	39.1610
		Kant et al. [26]	2.2800	—	13.7500	43.4880
		Sayyad and Ghugal [27]	2.7970	2.3910	12.4630	39.5690
10	5	Present theory ($\varepsilon_z \neq 0$)	6.2694	209.0304	3.1130	169.5280
		Avhad and Sayyad [28]	5.8645	205.2050	3.0862	169.2986
	10	Present theory ($\varepsilon_z \neq 0$)	6.2696	121.4089	3.1130	169.4032
		Avhad and Sayyad [28]	5.8645	119.2910	3.0863	169.1772
	20	Present theory ($\varepsilon_z \neq 0$)	6.2697	73.7323	3.1130	169.3324
		Avhad and Sayyad [28]	5.8645	72.5438	3.0863	169.1176
	∞	Present theory ($\varepsilon_z \neq 0$)	6.2697	23.4787	3.1130	169.2752
		Avhad and Sayyad [28]	5.8645	23.2686	3.0863	169.0576
		Reddy [10]	5.2870	23.2400	3.0920	168.1300
		Kant et al. [26]	5.2400	—	3.3300	172.6000
		Sayyad and Ghugal [27]	5.2650	23.0300	3.1000	168.7600
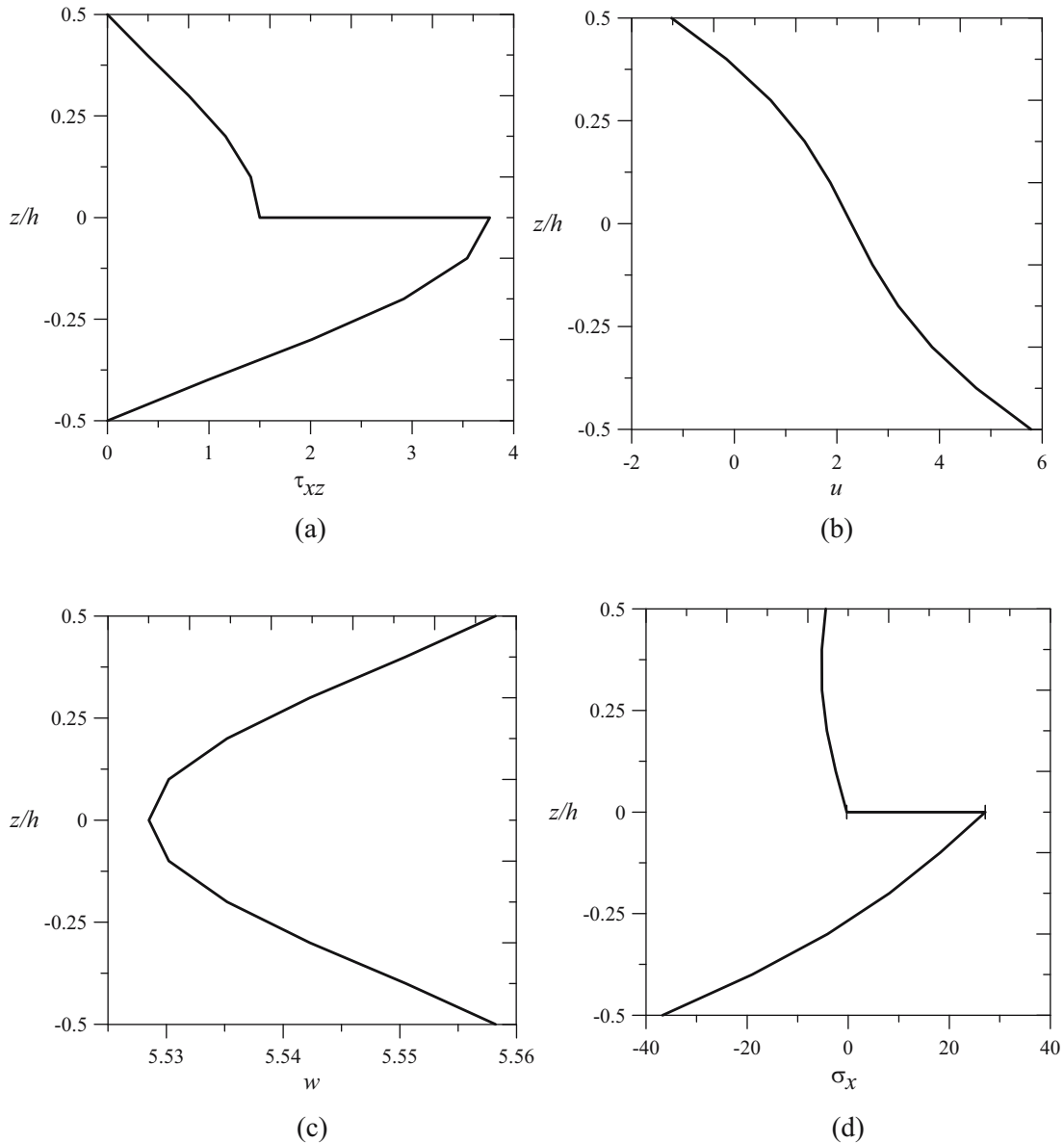
Figure 2: Variation through the thickness for transverse shear stresses (a), axial displacements (b), transverse displacements (c), and axial bending stresses (d) for antisymmetric two-layered (0°/90°) composite arches subjected to UDL ($R/h = 5$; $L/h = 4$).

antisymmetric two-layered (0°/90°) composite, and sandwich (0°/Core/0°) arches. Table 2 shows the material properties used in the present theory. The present theory obtained more accurate results than other theories for two-layered and three-layered composite and sandwich arches.

The overall depth of the arches through the thickness is assumed to be unity and other dimensions depend upon the aspect ratios (L/h) and (R/h). The present theory used the non-dimensional considerations as given below.

$$\overline{w} = 100 \frac{E_3 h^3}{q_0 L^4} w\left(\frac{L}{2}\right), \tag{40}$$

$$\overline{u} = \frac{E_3}{q_0 h} u\left(0, -\frac{h}{2}\right), \tag{41}$$

$$\overline{\sigma}_x = \frac{h}{q_0} \sigma_x\left(0, -\frac{h}{2}\right), \tag{42}$$

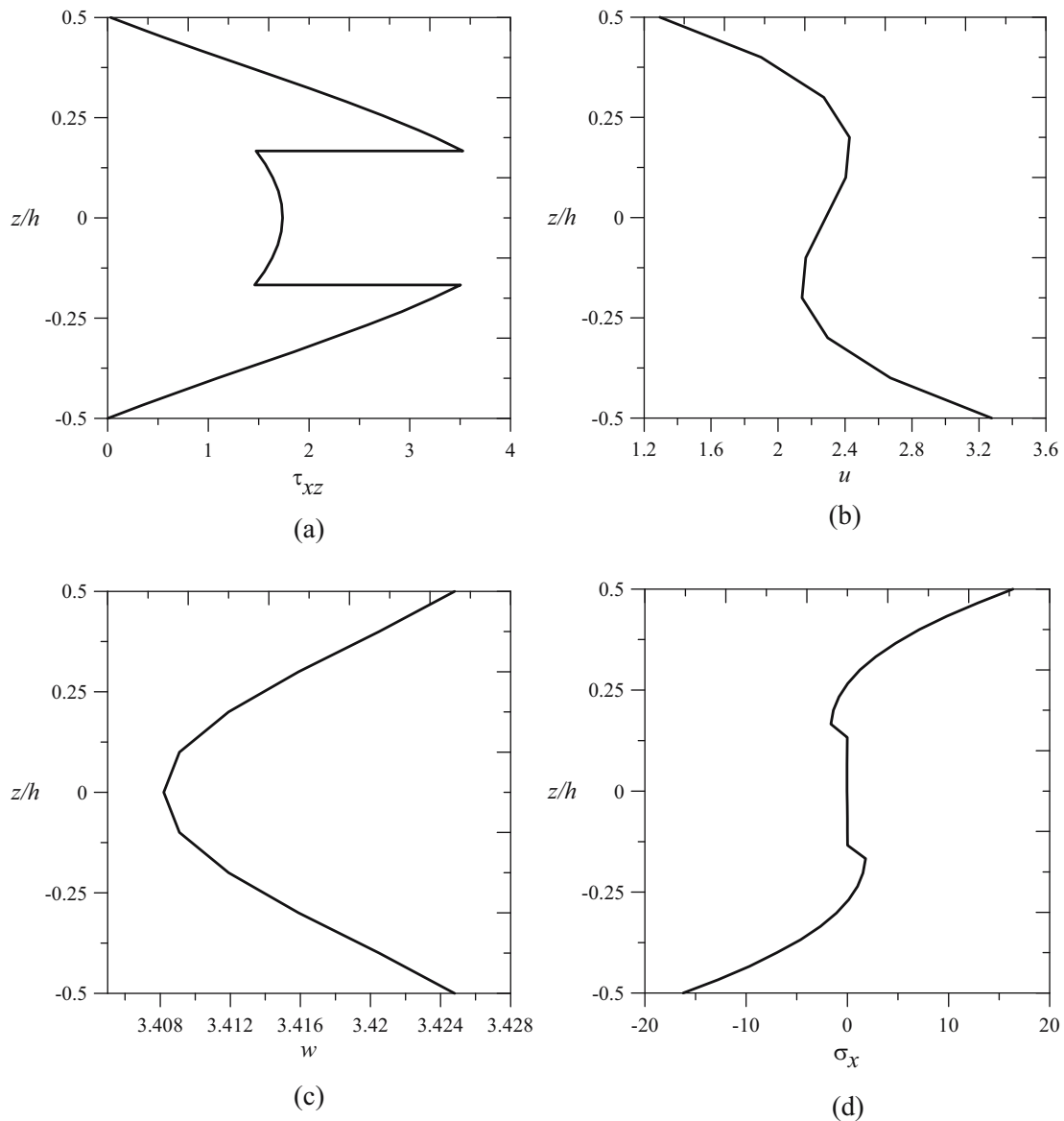$$\overline{\tau}_{xz} = \frac{\tau_{xz}}{q_0}(0, 0), \tag{43}$$

Figure 3: Variation through the thickness for transverse shear stresses (a), axial displacements (b), transverse displacements (c), and axial bending stresses (d) for symmetric three layered (0°/90°/0°) composite arches subjected to UDL ($R/h = 5$; $L/h = 4$).

where $\overline{w}$, $\overline{u}$, $\overline{\sigma}_x$, and $\overline{\tau}_{xz}$ are non-dimensional terms such as transverse displacements, axial-displacements, bending stresses, and transverse shear stresses used for various lamination schemes (0°/90°, 0°/90°/0°, and 0°/Core/0°). In case of antisymmetric as well as symmetric layered composite arches, each layer has equal thickness. But in case of sandwich arches, top face sheet and bottom face sheet have thickness 0.1 times that of the total thickness of arches, and the middle soft core has a thickness 0.8 times that of total thickness of the arches.

Table 3 shows the assessment of non-dimensional results such as transverse shear stresses, axial displacements, transverse displacements, and axial bending stresses

for antisymmetric two-layered composite (0°/90°) arches subjected to UDL. The present results match well with that obtained by Avhad and Sayyad [28] for curved beams for transverse shear stresses, axial displacements, and transverse displacements at aspect ratio, *viz.*, $L/h = 4$ and 10; the ratio between radius of curvature and total thickness of arches is formulated as $R/h = 5$, 10, 20, and ∞. It is observed that present results closely matches with that in previous study [28] for axial displacements through the thickness, somewhat improved in case of transverse shear stresses and slightly deficient in case of transverse displacements and axial bending stresses at $L/h = 4$ and $R/h = 5$.
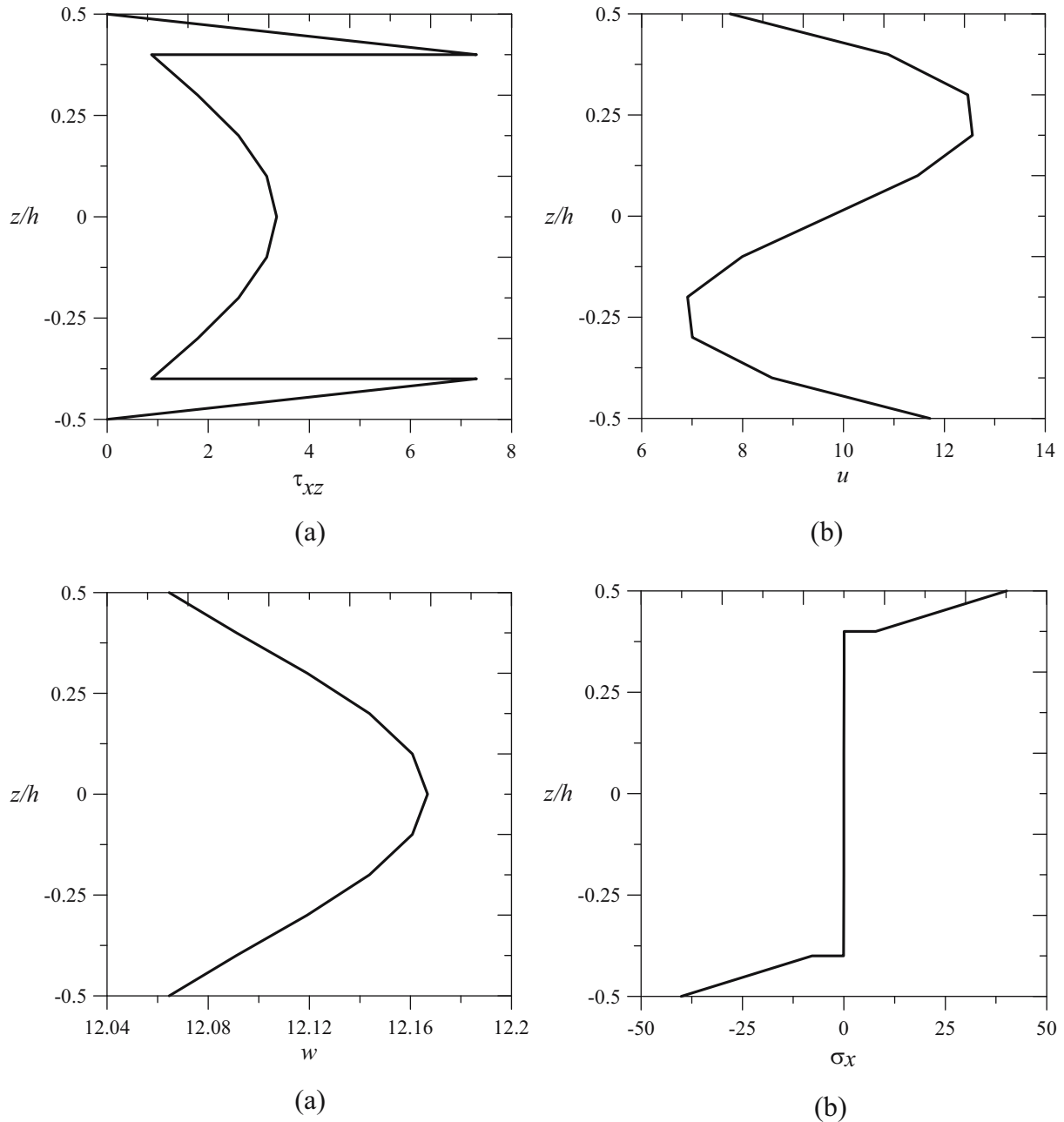
Figure 4: Variation through the thickness for transverse shear stresses (a), axial displacements (b), transverse displacements (c), and axial bending stresses (d) for sandwich (0°/Core/0°) arches subjected to UDL ($R/h = 5$; $L/h = 4$).

Table 3 presents the static responses of antisymmetric two-layered composite arches subjected to UDL, *i.e.*, bending stresses. The maximum value of axial bending stresses is noted at the top surface of arches, *i.e.*, $z = -h/2$ and fibers are placed in 0° layer horizontally along the length of the arches, at aspect ratio $L/h = 4$ and $R/h = 5$. When transverse load is applied uniformly distributed over the length of the arches, the fibers in the abovementioned layer reach the extreme ends through the thickness and give

rise to maximum value of bending responses. The minimum value of axial bending stresses is noticed at the bottom fiber of arches, *i.e.*, $z = +h/2$ and fibers are laid in 90° layer, which is perpendicular to 0° layer at aspect ratio $L/h = 4$ and $R/h = 5$. Under such loading, the fibers are not extendable more in the 90° layer and give rise to minimum value of bending stress at the same aspect ratio. At the interference of layers or neutral axis of arches, two values of bending stresses are available as shown in Figure 2. Present results are compared

with those published by Reddy [10], Kant *et al.* [26], Sayyad and Ghugal [27], and Avhad and Sayyad [28] for straight beams only (L/h = 4 and 10 and $R = \infty$).

Figure 2 shows variation through the thickness for normalized transverse shear stresses, normalized axial displacements, normalized transverse displacements, and normalized axial bending stresses for antisymmetric two-layered composite arches subjected to UDL. The maximum value of transverse shear stresses is noted at $z/h = 0$ and satisfies zero boundary conditions at top and bottom surfaces of the arches. The minimum value of transverse shear stresses is noted at the top and bottom fibers of the arches when subjected to UDL. The maximum normalized axial displacements are noted in the top surface of the arches when fibers are placed in 0° layers and minimum normalized axial displacements are accounted in 90° layers of the arches.

The axial displacements change their sign from positive to negative. The transverse displacements vary linearly through the thickness of arches subjected to UDL. According to the theory of Bernoulli [1], Timoshenko [3,4], and Reddy [10], transverse displacements are constants through the thickness. But present exponential theory revealed that non-dimensional transverse displacements are not constant through the thickness. It is noticed that present results are in good agreement with those obtained by Sayyad and Ghugal [27] and Avhad and Sayyad [28] for the mentioned cases ($R = \infty$ and $R \neq \infty$).

It is observed that if the aspect ratio increases, very minute variations observed in the non-dimensional values. Because increasing aspect ratio leads to thinning of arches. Hence, presented results are validated for thick arches having aspect ratios L/h = 4 and L/h = 10, *i.e.*, for thick arches subjected to UDL. Transverse shear stresses satisfy zero boundary conditions at the bottom and top fiber of layered composite (0°/90°) arches subjected to UDL.

Table 4 shows that assessment of non-dimensional results containing axial displacements, transverse shear stresses, vertical displacements, and axial bending stresses for symmetric three layered (0°/90°/0°) composite arches subjected to UDL. Present theory results are in good agreement with those published by Avhad and Sayyad [28].

It is observed that the bending responses through the thickness are closely matches with the results presented by Avhad and Sayyad [28]. It is noticed that variation in non-dimensional bending stresses through the thickness for antisymmetric three-layered composite arches is found to be truthfulness due to curvature in action.

Figure 3 shows variations through the thickness of normalized transverse shear stresses, normalized axial displacements, transverse displacements, and axial bending stresses for symmetric three-layered composite arches subjected to UDL, for aspect ratios such as L/h = 4 and 10 and R/h = 5, 10, 20,....∞. For straight layered beams, results are obtained and compared with earlier published results for $R = \infty$.

Minimum value for normalized vertical displacements was noted for symmetric three-layered (0°/90°/0°) composite arches due to the absence of extension axial bending coupling stiffness. The maximum value for normalized vertical displacements is noted at deep curvature, and minimum at shallow curvature, *i.e.*, radius of curvature of arches increases with the decrease in the non-dimensional vertical displacements and *vice versa*.

It is also observed that non-dimensional transverse displacements are varying through the thickness. Considering the thickness stretching effect, *i.e.*, transverse normal strain, axial displacements vary and change their sign through the total thickness of arches. In some classical theories like Bernoulli [1], Timoshenko [3,4], and Reddy [10], this effect was neglected. The transverse shear stresses satisfy zero boundary conditions at bottom and top fiber of layered composite (0°/90°/0°) arches subjected to UDL. Table 5 shows that the normalized transverse shear stresses satisfy zero boundary condition at the top fiber of arches and bottom fiber of sandwich (0°/Core/0°) arches. The results are found to be very prominent than other theories.

From the Figure 4, it is observed that the non-dimensional transverse displacement is remains constant through the thickness due to considering the thickness stretching effect, *i.e.*, $\varepsilon_z \neq 0$ and hence, it is closely matches with Avhad and Sayyad [28]. But in some renowned theories such as Bernoulli [1], Timoshenko [3,4], and Reddy [10], transverse displacements are more improved than present theory. Those theories have not captures well numerical results because of ignorance of thickness stretching effect, *i.e.*, $\varepsilon_z = 0$.

Figure 4 shows the variations through the thickness of transverse displacements, normalized axial displacements, transverse shear stresses, and axial bending stresses for sandwich (0°/Core/0°) arches for aspect ratios such as L/h = (4 and 10) and R/h = 5, 10, 20, ∞. Present results are compared with earlier published results at $R = \infty$ only for straight layered beams. Maximum normalized transverse shear stresses are obtained in 0° layer at top and bottom face sheets of sandwich arches. The minimum value of non-dimensional shear stresses is obtained at middle-soft-core

for sandwich arches. The maximum value of normalized transverse displacements is noted at deep curvature and minimum is noted at shallow curvature for sandwich arches due to the presence of extension bending coupling stiffness.

4 Conclusion

The present theory developed an accurate exponential normal and shear deformation theory and explored the static responses for antisymmetric two-layered, symmetric three-layered composite and sandwich arches subjected to UDL. The present theory accounted for the effects of transverse shear deformation and normal deformation. The present theory does not require any shear correction factor to satisfy zero traction free transverse shear stresses conditions at bottom and top fibers of arches.

Navier-type closed form solution is applicable to only SS end boundary conditions. The numerical results concerned with axial/transverse displacements and bending/shear responses are obtained efficiently and more accurately than other theories. The present exponential shear deformation and normal deformation theory of layered composite and sandwich arches can be set as standard solution for forthcoming researchers. Therefore, the thickness stretching effect plays a vital role while predicting bending responses for sandwich and layered composite arches.

Nomenclature

b	unit width for arched beam ($b = 1.0$)
CBT	classical beam theory
E_1, E_3	modulus of elasticity of (1, 3) laminate plane
FSDT	first-order shear deformation theory
$\{f\}$	force vector
G_{13}, G_{23}	shear modulus of the respective lamina
HSDTs	higher order shear deformation theories
h	total thickness of arches
$[K]$	stiffness matrix
m	+ve integer varying with the odd number ($m = 1, 3, 5, 7 \ldots\infty$)
q_0	maximum intensity of the UDL loading
Q_{ij}	transformed rigidity matrix

SS	simply supported
TBT	Timoshenko beam theory
UDL	uniformly distributed loading
$\{\Delta\}$	unknown variables
ε_z	normal deformation effect
γ_{xz}	shear deformation effect
σ	stress quantity
ε	strain quantity
ρ	density of the material
δ	variational operator
u_0, w_0, ϕ and ψ	unknown displacement function at mid-plane of beam
$\overline{\tau}_{xz}, \overline{u}, \overline{w}, \overline{\sigma}_x$	non-dimensional terms *viz*. bending stresses and transverse shear stresses
μ_{13}, μ_{31}	Poisson's ratios

References

[1]   Bernoulli J. Curvatura laminae-elasticae. Acta Eruditorum Lipsiae. 1694;34:262–76.

[2]   Euler L. Methodus inveniendi lineas curvas maximi minimive proprietate gaudentes. Lousanne/Geneva, Switzerland: Marcum-Michaelem Bousquet & Socios. 1744.

[3]   Timoshenko SP. On the correction for shear of the differential equation for transverse vibrations of prismatic bars. Philos Mag Ser 1. 1921;41:744–6.

[4]   Timoshenko SP. On the transverse vibrations of bars of uniform cross-section. Lond Edinb Dublin Philos Mag J Sci. 1922;43:125–31.

[5]   Sayyad AS, Ghugal YM. On the free vibration analysis of laminated composite and sandwich plates: A review of recent literature with some numerical results. Compos Struct. 2015;129:177–201.

[6]   Sayyad AS, Ghugal YM. Bending, buckling and free vibration of laminated composite and sandwich beams: A critical review of literature. Compos Struct. 2017;171:486–504.

[7]   Sayyad AS, Ghugal YM. Modeling and analysis of functionally graded sandwich beams: A review. Mech Adv Mater Struct. 2019;26(21):1776–95.

[8]   Kant T, Manjunath BS. Refined theories for composite and sandwich beams with C^0 finite elements. Comput Struct. 1989;33(3):755–64.

[9] Aitharaju VR, Averill RC. C^0 Zig-zag finite element for analysis of laminated composite beams. J Eng Mech. 1999;125(3):323–30.

[10] Reddy JN. A simple higher-order theory for laminated composite plates. J Appl Mech. 1984;51(4):745–52.

[11] Khdeir AA, Reddy JN. An exact solution for the bending of thin and thick cross-ply laminated beams. Compos Struct. 1997;37(2):195–203.

[12] Khdeir AA, Reddy JN. Free and forced vibration of cross-ply laminated composite shallow arches. Int J Solids Struct. 1997;34(10):1217–34.

[13] Carrera E. Transverse normal stress effects in multilayered plates. J Appl Mech. 1999;66(4):1004–12.

[14] Carrera E. A study of transverse normal stress effect on vibration of multilayered plates and shells. J Sound Vib. 1999;225:803–29.

[15] Carrera E. Transverse normal strain effect on thermal stress analysis of homogeneous and layered plates. AIAA J. 2005;43(10):2232–42

[16] Zenkour AM. Maupertuis-Lagrange mixed variational formula for laminated composite structures with a refined higher-order beam theory. Int J Non-linear Mech. 1997;32(5):989–1001.

[17] Sayyad AS, Ghugal YM. Flexure of thick beams using new hyperbolic shear deformation theory. Int J Mech. 2011;5(3):113–22.

[18] Sayyad AS, Ghugal YM. A sinusoidal beam theory for functionally graded sandwich curved beams. Compos Struct. 2019;226:111246.

[19] Sayyad AS, Avhad PV. On static bending, elastic buckling and free vibration analysis of symmetric functionally graded sandwich beams. J Solid Mech. 2019;11(1):166–80.

[20] Avhad PV, Sayyad AS. Static analysis of functionally graded composite beams curved in elevation using higher order shear and normal deformation theory. Mater Today Proc. 2020;21(2):1195–9.

[21] Avhad PV, Sayyad AS. On the static deformation of FG sandwich beams curved in elevation using a new higher order beam theory. Sadhana. 2020;45:1–16.

[22] Tornabene F, Fantuzzi N, Bacciocchi M. Refined shear deformation theories for laminated composite arches and beams with variable thickness: Natural frequency analysis. Eng Anal Bound. 2019;100:24–47.

[23] Dimitri R, Tornabene F. A parametric investigation of the seismic capacity for masonry arches and portals of different shapes. Eng Fail Anal. 2015;52:1–34.

[24] Tornabene F, Dimitri R, Viola E. Transient dynamic response of generally-shaped arches based on a GDQ-time-stepping method. Int J Mech Sci. 2016;114:277–314.

[25] Tornabene F, Dimitri R. A numerical study of the seismic response of arched and vaulted structures made of isotropic or composite materials. Eng Struct 2018;159:332–66.

[26] Kant T, Pendhari SS, Desai YM. On accurate stress analysis of composite and sandwich narrow beams. Int J Comput Methods Eng. 2007;8(3):165–77.

[27] Sayyad AS, Ghugal YM. Effect of thickness stretching on the static deformations, natural frequencies, and critical buckling loads of laminated composite and sandwich beams. J Braz Soc Mech. 2018;40(6):296.

[28] Avhad PV, Sayyad AS. On the deformation of laminated composite and sandwich curved beams. Curved Layer Struct. 2021;9(1):1–12.